



Published in final edited form as:

Int J Cancer. 2012 January 1; 130(1): 190–199. doi:10.1002/ijc.25978.

The preclinical therapeutic response of residual metastatic disease is distinct from its primary tumor of origin

Chi-Ping Day¹, John Carter², Carrie Bonomi², Melinda Hollingshead^{3,4}, and Glenn Merlino^{1,4}

¹ Laboratory of Cancer Biology and Genetics, National Cancer Institute, Bethesda, MD, USA

² Developmental Therapeutics Program, SAIC-Frederick, Inc., National Cancer Institute-Frederick, Frederick, MD, USA

³ Developmental Therapeutics Program, Division of Cancer Treatment and Diagnosis, NCI-Frederick, Frederick, MD, USA

Abstract

Cancer-related deaths are caused principally by recurrence and metastasis arising from residual disease, whose therapeutic responses has been suggested to be substantially different from primary tumors. However, experimental animal models designed for evaluating the therapeutic responses of residual disease are mostly lacking. To overcome this deficiency, we have developed a preclinical model that recapitulates the progression for advanced non-small cell lung cancer (NSCLC). An archived Lewis Lung Carcinoma mouse tumor, propagated only through serial *in vivo* transplantation and never adapted to cell culture, was stably labeled using lentivirus-encoded biomarkers, consistently expressed through an RNA polymerase II promoter. Labeled tumors were inoculated into syngeneic immunocompetent mice to ensure superior tumor-host interactions. Primary tumors were resected upon reaching a predetermined size, following by treatment in a setting akin to post-surgical first-line adjuvant chemotherapy and routine imaging to monitor the progression of pulmonary metastasis. We discovered that efficacious treatment, instead of reducing disease growth rates, significantly prolonged disease-free survival (DFS) and overall survival (OS). As in the clinic, cisplatin-based regimes were more effective in this model. However, the response of metastases to specific agents could not be predicted from, and often opposed, their effects on subcutaneous “primary” tumors, possibly due to their distinct growth kinetics and host interactions. We here introduce a clinically relevant model of residual metastatic disease that may more accurately predict the therapeutic response of recurrent, metastatic disease.

Introduction

Mouse models play a pivotal role in the development of anticancer drugs. Unfortunately, more than 70% of new oncological drugs fail to demonstrate activity in phase II trials¹. The value of current preclinical mouse models has therefore been seriously questioned. Thus, development of new preclinical models exhibiting enhanced predictive powers with respect to clinical outcome remains a research priority.

Mice bearing human tumor xenografts have become the standard in preclinical cancer modeling based on their clinically relevant cancer histopathologies, as well as advantages in

Correspondence: Glenn Merlino, PhD, Laboratory of Cancer Biology and Genetics, National Cancer Institute, NIH, Building 37, Room 5002, 37 Convent Drive, Bethesda, MD 20892-4264 USA, Phone: (301) 496-4270, Fax: (301) 480-7618, gmerlino@helix.nih.gov. ⁴To whom correspondence should be addressed: Glenn Merlino – gmerlino@helix.nih.gov; Melinda Hollingshead - hollingm@mail.nih.gov.

progression tracking, testing efficiency and statistical power. However, human cells must be transplanted into mice lacking a fully functional immune system, known to be critically involved in tumor development and progression. In this type of model, tumor growth delay is frequently used as the endpoint for accessing drug activity², and death is usually defined by the tumor burden reaching protocol-set limits, rather than disease-associated mortality³. In contrast, in clinical studies, therapeutic response requires tumor shrinkage or stable disease⁴, and overall survival time must be followed after treatment to assess the full life expectancy and the possibility of disease recurrence.

Critically, currently available preclinical models using human cancer xenografts fail to incorporate disease progression and metastasis, seriously limiting their relevance to the clinic. In clinical practice, surgical resection is the primary choice of treatment for many types of tumors, especially in their early stage. However, tumor cells may have already disseminated and survived as occult residual disease that can remain in “clinical dormancy” for years⁵. Once these cells break quiescence for reasons currently unknown they can grow into clinically significant macrometastases, which are ultimately responsible for the majority of cancer-related deaths. Therefore, post-surgery adjuvant therapies are often initiated to prevent or control recurrent and/or metastatic disease. The biology of advanced stage cancer progression is distinct from primary tumor growth⁶ and has been beyond the capacity of current preclinical cancer model to adequately address.

Here we aimed to develop a more clinically relevant mouse model of cancer progression and metastasis to help address these issues. Mouse Lewis Lung Carcinoma (LLC), recently used in a number of high-profile preclinical studies⁷⁻⁹, was chosen as a model of metastatic non-small cell lung carcinoma (NSCLC). To avoid alterations associated with adaptation to *in vitro* culture, we employed archived LLC tissue that had been maintained only through serial transplantation, hereafter referred to as LLCCom (LLC Only in Mice). For tracking disease progression, a tumor must be labeled with bioimaging markers; however, such attempts often fail because high expression of commonly used xenobiotic markers, including green fluorescence protein (GFP) and luciferase (Luc), can induce an immune response, resulting in tumor rejection or unsustainable monitoring^{10, 11}. Previously, we reported that the RNA polymerase II promoter (Pol2), which exhibits relatively low transcriptional activity, maintains more sustainable and consistent biomarker expression in immunocompetent mice. We therefore labeled the LLCCom tumor with a Pol2-Luc/GFP lentiviral vector via an *ex vivo* procedure¹², followed by transplantation into syngeneic immunocompetent mice to generate more appropriate tumor-host interactions. Upon reaching a pre-determined size the primary tumors were surgically resected followed by immediate chemotherapeutic treatment, a setting akin to adjuvant chemotherapy. Host mice were monitored with bioluminescence (BL) imaging for disease progression. With this new model we were able to evaluate the response of residual metastatic disease to first-line NSCLC chemotherapy. We found that pulmonary residual disease exhibited growth kinetics and therapeutic responses that were distinct from their subcutaneous counterparts. This spontaneous metastasis model may improve our ability to predict the efficacy of drugs for advanced-stage cancer patients.

Materials and Methods

Lentiviral vector

The lentiviral vector Pol2-Luc/GFP was described previously¹². The vector information is provided upon request to Dr. Dominic Esposito (e-mail: espositod@mail.nih.gov), NCI-Frederick, Frederick, MD, USA.

Animals

Six to eight week-old inbred albino C57BL/6 female mice (C57BL/6 c-Brd/c-Brd/Cr) mice were used to reduce bioluminescence absorption, cage mate fighting, and experiment variation. All mouse experiments were performed in accordance with Animal Study Protocols approved by the Animal Care and Use Committee (ACUC), NCI, National Institutes of Health (Please see Supplementary Information for institutional regulation of animal care).

Tumor labeling and *in vivo* cycling

The LLC tissue in this study was maintained in syngeneic C57BL/6 mice since its spontaneous appearance in the mouse lungs, and was cryopreserved in the tumor repository of NCI-Frederick in 1978. After being revived and expanded in C57BL/6 mice by subcutaneous transplantation, the tumor was infected *ex vivo* with Pol2-Luc/GFP lentivirus without cell culture or drug selection, as described previously¹², and then inoculated into C57BL/6 mice. Upon reaching 500 mm³, tumors were surgically removed, and lung metastasis was monitored periodically by intraperitoneal injection with 150 mg/kg of luciferin and BL imaging using a Xenogen IVIS system (Caliper Life Sciences, Alameda, CA). This transplantation was referred as passage 0 (P0). When the chest BL flux was higher than 10⁷ photon/sec, the mice were sacrificed to harvest the lungs. The labeled lung nodules were identified by *ex vivo* BL imaging, resected, and subcutaneously transplanted into mice (the first passage, P1). The same procedure was repeated once (P2), and the collected labeled lung nodules were then subcutaneously transplanted into twenty mice as the third passage (P3). When P3 tumors reached 500 mm³, they were collected into eighty tubes and frozen in liquid nitrogen as working stock. All the tumors in the following studies were expanded from the P3 working stock.

Preclinical model of spontaneous metastasis

For a preclinical study, a vial of P3 LLC tumor was expanded subcutaneously in ten mice (equals P4). The expanded tumors were resected at 500 mm³ and transplanted subcutaneously into required number of mice for the actual drug study (P5). For the model of spontaneous metastasis, the primary tumors were surgically removed at 500 mm³, and the mice randomized into treatment groups. The drugs used in this study were obtained from the Drug Synthesis & Chemistry Branch, DTP, NCI (Bethesda, MD, USA). The control group received vehicle solution, and the experimental group received treatments of chemotherapeutic agents (see Supplementary Methods for drug preparation), with dose and schedule specified in Results. In the combination therapy studies, each drug or its vehicle solution was given individually to the mice of the treated or control groups, respectively, according to its dosing schedule. The size of subcutaneous tumors was measured manually and calculated by $V \text{ (mm}^3\text{)} = 0.5 \times L \times W^2$, where L is length and W is width in mm. The metastasis or recurrence was monitored periodically by BL imaging with the Xenogen IVIS system, as described above. Determination of circulating anti-GFP antibody levels in mice, as well as tumor inhibition ratios are described in Supplementary Methods.

Pathological analysis

Harvested lungs were fixed in 10% formaldehyde and paraffin-embedded. The adjacent serial sections were stained with hematoxylin and eosin (H&E) for histological analysis, or used for GFP immunohistochemistry (ab6556, Abcam, Cambridge, MA, USA). Histopathology was provided by Dr. Miriam Anver (Pathology and Histotechnology Laboratory, SAIC, NCI-Frederick). For quantitative analysis, slides were scanned using the ScanScope XT system and images were analyzed by Spectrum Plus pathology analysis software (Aperio Technologies, Vista, CA).

Results

Establishing a traceable preclinical model for spontaneous NSCLC metastasis in immunocompetent mice

To generate a preclinical model with more appropriate tumor-host interactions, we used an archived LLC_{Com} tumor that had only been maintained *in vivo* in C57BL/6 mice. This LLC_{Com} tumor was labeled using our Pol2-Luc/GFP lentivirus vector through an *ex vivo* procedure, as described previously¹², and transplanted into albino C57BL/6 mice as passage 0 (P0). Reasoning that each nodule of spontaneous pulmonary metastasis arises clonally^{13, 14}, we used *in vivo* cycling to obtain a uniformly labeled, metastatic LLC_{Com} clone. The lung nodules collected at the third cycle (P3) were expanded in mice and stored in liquid nitrogen as the working stock. For all subsequent preclinical studies, a single vial of cryopreserved P3 tumor was retrieved, expanded once (P4), and transplanted into the required number of mice (P5) for experiments.

To determine the labeling consistency *in vivo*, we measured the ratio of BL intensity to tumor size (BL/size) as a normalized reporter activity at each passage¹². As shown in Fig. 1A (left panel), the median BL/size decreased from the initial inoculation (P0) into P1, but then increased from P1 to P3 in accordance with clonal enrichment. Thereafter the ratio was consistently maintained (P4 and P5), indicating that the labeling was stable and sustainable. Immunohistochemical staining showed that GFP was uniformly, albeit relatively weakly, expressed in the cytoplasm of LLC_{Com} cells in the lungs of P5 mouse, corroborating the advantage of *in vivo* cycling (Fig. 1A, right panels). As expected, GFP staining was absent from normal lung tissue. This result suggested that this LLC_{Com} clone expressed sufficient but relatively low reporter activity, allowing its identification by BL imaging, yet minimizing host immunity against foreign biomarkers¹⁰⁻¹². To test this hypothesis, we challenged the mice using LLC tumors labeled with either Pol2-Luc/GFP or FerH-Luc/GFP vector, whose promoter activity is comparable to that of the standard CMV promoter¹², then measured circulating GFP antibodies in mice. No anti-GFP antibody was detected in the sera of the Pol2-Luc/GFP group, whereas substantial levels ($7.89 \pm 1.93 \mu\text{g/ml}$) were detected in FerH-Luc/GFP mice, in agreement with previous data showing that Pol2-Luc-GFP labeling is more consistent and sustainable than FerH-Luc-GFP in syngeneic C57BL/6 mice¹².

To optimize the metastatic occurrence LLC_{Com} fragments were subcutaneously inoculated into four groups of mice, and the tumors resected when their sizes reached 125, 250, or 500 mm³, followed by BL monitoring for pulmonary metastasis (Fig. 1B). When the resection size was 500 mm³ metastases were detected in more than 80% of mice within six days. In the following seven days (day 6 to 13) the chest BL level in every mouse significantly increased and the occurrence of pulmonary metastasis reached 100%. When tumors were resected at 125 or 250 mm³ the pulmonary metastases occurred later with significantly lower incidence (Fig. 1B). We concluded that resection at 500 mm³ provided robust and consistent occurrence of spontaneous pulmonary metastasis (>90%); this model was therefore used for all subsequent studies.

According to the current NSCLC staging system, pulmonary metastases are categorized as T4/M1 disease at stage IIIB/IV¹⁵⁻¹⁷; therefore, our LLC_{Com} metastasis model is relevant to metastatic NSCLC at stage IIIB/IV. Metastatic LLC_{Com} lesions were also observed outside the lung in this model (Supplementary Fig. S1); however, their development was prematurely terminated by lethally aggressive pulmonary metastases¹⁸. Other techniques demonstrated the potential of this tumor to metastasize to common NSCLC sites. Direct injection of LLC_{Com} cells into the right lower lobe of the lungs resulted in metastatic spread to other lobes (Supplementary Fig. S2). Cardiac injections produced metastases in the brain, adrenal gland and lymph nodes at multiple sites, as well as lungs (Supplementary Fig. S3).

These results demonstrate that murine LLC is capable of metastasizing to organs commonly targeted by human NSCLC. In our current model, subcutaneous inoculation allows resection of primary tumors at a pre-determined size, providing a reasonable window for monitoring progression and the therapeutic response of metastases.

Quantitative monitoring of metastatic progression in the LLCom model

To determine if BL correlated with disease progression, subcutaneous LLCom tumors were resected at 500 mm³, and mice randomly selected every 2 to 4 days for BL imaging *in vivo* (Upper panel Fig. 2A), followed by lung harvest for histopathological analysis (lower panel, Fig. 2A). Total area of tumor nodules in each lung section quantified by digital image analysis served as an approximation of overall tumor burden. Although the overall distribution showed a two-phase pattern (Fig. 2B, left panel), the majority of mice (13/17) fell in the BL < 5×10⁷ region in which chest BL and overall pulmonary tumor area exhibited a tightly linear correlation (R² = 0.8034; right panel Fig. 2B). Therefore, we have identified the linear range in which *in vivo* BL tightly correlates with actual tumor burden in the lungs, allowing quantitative tracking of disease progression *in vivo*.

During this study, in no case were visible macrometastases (diameter ≥ 1 mm)⁷ found in mice with maximal chest BL levels consistently under 1.5×10⁵ photon/sec. In an independent experiment, all such mice, either in control or treated groups, remained healthy through the entire period of study (Supplementary Fig. S4). For purposes of *in vivo* monitoring a chest BL level of 1.5×10⁵ photon/sec was therefore considered the “macrometastatic threshold”; lung BL surpassing this threshold designated the onset of detectable macrometastasis and the end of the equivalent of clinical dormancy. The time from primary tumor resection to macrometastatic detection by BL and to death was defined as the disease-free survival (DFS) and overall survival (OS) period, respectively. Thus, our model allowed the adoption of clinically relevant parameters for data analysis. This correlation between chest BL and pulmonary tumor burden is summarized in Table 1.

Responses of pulmonary metastases to single-agent adjuvant chemotherapy

To evaluate the therapeutic responses of the LLCom tumor, we assessed the efficacy of paclitaxel, one of the most frequently used first-line NSCLC agents. We modified a reported procedure¹⁹ to develop a “humanized regime” to mimic pharmacokinetics of paclitaxel in clinical treatment: one-dose of 7.5 mg/kg of paclitaxel for five consecutive days, five days off, and a second cycle of five-day dosing (QDx5, 5D off, QDx5). This regime is well below the maximum tolerant dose (MTD) of paclitaxel for mice (22.5 mg/kg) that we have determined (data not shown).

The activity of this regime was first tested in the classic subcutaneous model. The treatment was initiated when the subcutaneous LLCom tumors reached 125 mm³ (day 6). In either group, all tumors began to grow immediately after inoculation (Fig. 3A), and paclitaxel uniformly reduced tumor growth (Fig. 3B). At day 13, tumor size in the treated group was significantly smaller than that in the control group (Fig. 3C). Accordingly, this treatment significantly reduced the tumor growth rate relative to control at the subcutaneous site (Fig. 3D). The experiment was terminated prior to the second dosing period at day 16 when the tumors in the control group reached protocol-defined limits; therefore, the long-term impact of tumor burden on host survival could not be evaluated. We concluded that the “humanized regime” of paclitaxel was able to delay the growth of subcutaneous tumors to a significant, albeit limited, extent.

Next, we tested the efficacy of this regime in the setting of post-surgical adjuvant chemotherapy. After resection of primary tumors at 500 mm³, mice were randomized to

receive either control vehicle or 7.5 mg/kg of paclitaxel, followed by BL monitoring. The time to metastatic onset was heterogeneous and unevenly distributed among individual mice, (Fig. 4A and B), as was the time to morbidity. Kaplan-Meier analysis showed that adjuvant paclitaxel treatment significantly extended the post-surgery OS (18 days vs. 15 days in control; $p = 0.0004$; Fig. 4C) and DFS (6 days vs. 4 days in control; $p = 0.0268$). Since studies have shown that it is possible to translate the time frame of cancer development between mouse and human²⁰, we estimated that 3 and 2 mouse days are equivalent to 4 and 2.67 human months, respectively. Based on its poor prognosis, prolonging median survival for late-stage NSCLC patients by three to six months would be considered clinically significant²¹.

In contrast to the subcutaneous tumor (Fig. 3C), paclitaxel treatment had no significant effect on the disease growth rate of pulmonary metastases (Fig. 4D, right panel). These results suggest that, for recurrent metastatic disease, efficacious treatment delays the time of disease onset rather than slowing the growth rate.

Preclinical evaluation of relevant drug combinations as adjuvant chemotherapy for residual metastatic disease

To further explore if the treatment efficacy for residual disease depends on the extension of DFS, we expanded the study to include multiple drugs and their combinations. Taxane- and platinum compound-based regimes are first-line therapies of advanced NSCLC²². Most antiangiogenic agents that have recently been introduced as cancer treatment have yielded higher activity when combined with conventional chemotherapy²³. Therefore, we tested the responses of metastatic disease to paclitaxel (PT), cisplatin (CDDP), and TNP470 (TNP), an angiogenesis inhibitor²⁴. They were administered singly or in combinations for eight regimes, and their doses and schedules adjusted to minimize the additive toxicity (Fig. 5A). Regression analysis demonstrated that DFS highly correlated with OS among all eight groups (Fig 5B, left panel). In contrast, no significant correlation was found between growth rates and OS (Fig. 5B, right panel). Indeed, for all efficacious treatments (CDDP, PT+TNP, and PT+CDDP+TNP), the OS was prolonged in proportion to the DFS. Our results suggest that onset time is a critical factor for the progression and therapeutic response of residual disease, and that DFS can serve as a surrogate marker of survival duration. Cisplatin and the PT+CDDP+TNP combination were the two most efficacious regimes with respect to extension of OS, and CDDP+TNP extended DFS, consistent with many clinical studies showing that cisplatin-based regimes are relatively effective treatments for NSCLC.

Growth delay of tumors at the subcutaneous site is not predictive for drug response of residual metastatic disease

In contemporary preclinical studies, the efficacy of anti-cancer drugs is often evaluated by their ability to delay growth of primary tumors in mice. However, in clinical trials, which recruit patients with advanced-stage cancers, drugs are evaluated by their ability to prolong survival. To address if the effect of drugs on primary tumor growth can predict therapeutic responses of residual disease, we compared the responses of subcutaneous tumors and residual metastatic diseases within the same therapeutic setting.

LLCom tumors were subcutaneously inoculated into mice. When they reached 125 mm³ the same regimes as those in Fig. 5A were initiated. Cisplatin, paclitaxel and their combination had no significant effect, TNP470 and its combination with either paclitaxel or cisplatin significantly delayed growth, and the triple combination demonstrated the strongest growth delay (Fig. 5C, left panel). The efficacy of each treatment was quantified by calculating the tumor inhibition ratio, which represents the percentage of growth delay relative to control. The association between tumor inhibition ratios from the subcutaneous tumor model and the

OS interval taken from the spontaneous metastasis model (Fig. 5B), both under the same regimes, was further examined by regression analysis. As shown in Fig. 5C (right panel) no correlation existed, either positively or negatively, indicating that inhibition ratio or growth delay in subcutaneous tumor model cannot predict drug efficacy for residual metastatic disease.

At the end point of this experiment (day 18), we examined the lungs of each mouse by *ex vivo* BL imaging and found pulmonary metastasis in all groups. The lung BL distribution in each group was not overtly different from that found in the post-surgery treatment model (Fig. 5B), indicating that in this model neither the presence of the primary tumor nor surgical intervention significantly influenced the consequences of drug treatment for already-disseminated disease (Supplementary Fig. S5).

Discussion

The vast majority of preclinical studies select new drugs to advance into clinical trials based on their ability to inhibit the growth of subcutaneous human tumor xenografts in an immunocompromised mouse. These data have not reliably predicted clinical activity, suggesting that current preclinical models are incapable of excluding clinically inactive agents from the potential candidates^{25, 26}. This can be attributed to several possible reasons. First, recipient mice of human cancer xenografts are deficient in at least some immune and/or inflammatory function, which plays a critical role in determining the therapeutic responses of cancers²⁷. In contrast, earlier preclinical studies using immunocompetent mice bearing syngeneic murine tumors, including LLC NSCLC³, had successfully selected many first-line chemotherapeutic agents still used in the clinic today, including paclitaxel and cisplatin²⁸. Second, human cancer cell lines used in xenograft models may have been altered during long-term *in vitro* culture. In contrast, tumors that had never been forced to adapt to growth on plastic dishes have been reported to better predict clinical activity^{29, 30}. Finally, tumors at orthotopic and metastatic sites are known to respond differentially to chemotherapeutic agents^{31, 32} compared to their subcutaneous counterparts. Recently, efforts have been made to improve mouse models using human cancer xenografts. For example, Vantuyghem et al. developed a mouse model using a metastatic human breast cancer xenograft, and found that the dietary supplement genisten could reduce pulmonary metastatic burden with or without primary tumor resection³³. Thalheimer et al. studied human colon cancer metastasis using intraportal injections, and identified tumor dissemination to bone marrow³⁴. Nude mice were used in both studies, and no bioimaging marker was employed, so outcomes were evaluated by necropsy.

Here we describe the development of a uniformly labeled LLCom tumor, passaged only in mice, for use as a preclinical model of residual metastatic NSCLC. The surgical resection of the primary tumor enabled efficient and consistent metastatic progression, and temporal alignment of treatment schedules. The sustained and consistent labeling achieved using the Pol2-driven reporter and *in vivo* cycling generated a linear correlation between chest BL and pulmonary tumor burden, allowing quantitative tracking of disease progression *in vivo*. This feature permitted us to define the macrometastatic BL threshold marking the transition from clinically insignificant residual disease to macrometastasis^{35, 36}. To our knowledge, these features have not been reported in other syngeneic immunocompetent mouse models of recurrent/metastatic disease.

Our studies using multiple drugs showed that prognosis correlated well with the time required to cross the macrometastatic threshold, with the most effective agents better able to delay the metastatic onset, extending what would be the equivalent to clinical dormancy. This explains in part why DFS can serve as a surrogate marker for OS. This conclusion is

supported by preclinical and clinical studies of advanced stage cancers^{37–39}. For example, in an orthotopic syngeneic mouse model of osteosarcoma post-surgery adjuvant chemotherapy prolonged DFS and OS⁴⁰. A clinical study of NSCLC reported that chemotherapy can prolong DFS, but had no effect if lymph node metastases were already present⁴¹. The difference in therapeutic response between residual metastatic disease and subcutaneous tumors in our model can be attributed to their growth kinetics. Subcutaneous tumors grow uniformly following inoculation, and the experimental end point is determined by the growth rate. In contrast, efficacious treatment delays the onset of residual metastatic disease. After its onset, the disease growth rate had minimal influence on therapeutic outcome. Therefore, standard preclinical studies using subcutaneous tumor models may overlook drugs able to prevent residual disease progression without growth-inhibiting activity.

In conclusion, we have developed a novel preclinical mouse model focusing on the advanced cancer stages of recurrence and metastasis. The incorporation of appropriate tumor-host interactions and quantitatively consistent *in vivo* monitoring in our model should permit the adoption of more clinically relevant outcome criteria for drug studies, thereby enhancing their predictive power. We anticipate that this model will be valuable for testing new drugs and studying mechanisms of cancer progression. Future models can be modified by incorporating orthotopic transplantation of primary tumors, as well as using *in vivo* tumors derived from genetically engineered mice to build metastatic disease models with tailor-made genetic lesions.

Supplementary Material

Refer to Web version on PubMed Central for supplementary material.

Acknowledgments

C-PD is a recipient of the 2007 NCI Director's Innovation Award. The authors wish to thank Drs. Chand Khanna (Pediatric Oncology Branch, NCI, NIH), Elise Kohn and Phillip Dennis (Medical Oncology Branch, NCI, NIH) for useful discussions, and Drs. Betty Conde-Ortiz and Dominic Esposito (Advanced Technology Program, NCI-Frederick) for producing lentiviral vectors. The authors also thank Drs. Josh Webster and Mark Simpson (Laboratory of Cancer Biology and Genetics, NCI, NIH) and Dr. Agnes Holzbauer (Laboratory of Experimental Carcinogenesis, NCI, NIH) for kind help in pathological image analysis.

References

1. Sharpless NE, Depinho RA. The mighty mouse: genetically engineered mouse models in cancer drug development. *Nat Rev Drug Discov.* 2006; 5:741–54. [PubMed: 16915232]
2. Teicher BA. Tumor models for efficacy determination. *Mol Cancer Ther.* 2006; 5:2435–43. [PubMed: 17041086]
3. Talmadge JE, Singh RK, Fidler IJ, Raz A. Murine models to evaluate novel and conventional therapeutic strategies for cancer. *Am J Pathol.* 2007; 170:793–804. [PubMed: 17322365]
4. Therasse P, Arbuck SG, Eisenhauer EA, Wanders J, Kaplan RS, Rubinstein L, Verweij J, Van Glabbeke M, van Oosterom AT, Christian MC, Gwyther SG. New guidelines to evaluate the response to treatment in solid tumors. European Organization for Research and Treatment of Cancer, National Cancer Institute of the United States, National Cancer Institute of Canada. *J Natl Cancer Inst.* 2000; 92:205–16. [PubMed: 10655437]
5. Townson JL, Chambers AF. Dormancy of solitary metastatic cells. *Cell Cycle.* 2006; 5:1744–50. [PubMed: 16861927]
6. Langley RR, Fidler IJ. Tumor cell-organ microenvironment interactions in the pathogenesis of cancer metastasis. *Endocr Rev.* 2007; 28:297–321. [PubMed: 17409287]
7. Gao D, Nolan DJ, Mellick AS, Bambino K, McDonnell K, Mittal V. Endothelial progenitor cells control the angiogenic switch in mouse lung metastasis. *Science.* 2008; 319:195–8. [PubMed: 18187653]

8. Shaked Y, Henke E, Roodhart JM, Mancuso P, Langenberg MH, Colleoni M, Daenen LG, Man S, Xu P, Emmenegger U, Tang T, Zhu Z, et al. Rapid chemotherapy-induced acute endothelial progenitor cell mobilization: implications for antiangiogenic drugs as chemosensitizing agents. *Cancer Cell*. 2008; 14:263–73. [PubMed: 18772115]
9. Shojaei F, Wu X, Zhong C, Yu L, Liang XH, Yao J, Blanchard D, Bais C, Peale FV, van Bruggen N, Ho C, Ross J, et al. Bv8 regulates myeloid-cell-dependent tumour angiogenesis. *Nature*. 2007; 450:825–31. [PubMed: 18064003]
10. Steinbauer M, Guba M, Cernaianu G, Kohl G, Cetto M, Kunz-Schughart LA, Geissler EK, Falk W, Jauch KW. GFP-transfected tumor cells are useful in examining early metastasis in vivo, but immune reaction precludes long-term tumor development studies in immunocompetent mice. *Clin Exp Metastasis*. 2003; 20:135–41. [PubMed: 12705634]
11. Stripecke R, Carmen Villacres M, Skelton D, Satake N, Halene S, Kohn D. Immune response to green fluorescent protein: implications for gene therapy. *Gene Ther*. 1999; 6:1305–12. [PubMed: 10455440]
12. Day CP, Carter J, Bonomi C, Esposito D, Crise B, Ortiz-Conde B, Hollingshead M, Merlino G. Lentivirus-mediated bifunctional cell labeling for in vivo melanoma study. *Pigment Cell Melanoma Res*. 2009; 22:283–95. [PubMed: 19175523]
13. Yamamoto N, Yang M, Jiang P, Xu M, Tsuchiya H, Tomita K, Moossa AR, Hoffman RM. Determination of clonality of metastasis by cell-specific color-coded fluorescent-protein imaging. *Cancer Res*. 2003; 63:7785–90. [PubMed: 14633704]
14. Talmadge JE, Wolman SR, Fidler IJ. Evidence for the clonal origin of spontaneous metastases. *Science*. 1982; 217:361–3. [PubMed: 6953592]
15. Oliaro A, Filosso PL, Cavallo A, Giobbe R, Mossetti C, Lyberis P, Cristofori RC, Ruffini E. The significance of intrapulmonary metastasis in non-small cell lung cancer: upstaging or downstaging? A re-appraisal for the next TNM staging system. *Eur J Cardiothorac Surg*. 2008; 34:438–43. discussion 43. [PubMed: 18502660]
16. Naruke T, Tsuchiya R, Kondo H, Asamura H, Nakayama H. Implications of staging in lung cancer. *Chest*. 1997; 112:242S–8S. [PubMed: 9337297]
17. Mountain CF. Revisions in the International System for Staging Lung Cancer. *Chest*. 1997; 111:1710–7. [PubMed: 9187198]
18. Onn A, Isobe T, Itasaka S, Wu W, O'Reilly MS, Ki Hong W, Fidler IJ, Herbst RS. Development of an orthotopic model to study the biology and therapy of primary human lung cancer in nude mice. *Clin Cancer Res*. 2003; 9:5532–9. [PubMed: 14654533]
19. Sparreboom A, van Tellingen O, Nooijen WJ, Beijnen JH. Nonlinear pharmacokinetics of paclitaxel in mice results from the pharmaceutical vehicle Cremophor EL. *Cancer Res*. 1996; 56:2112–5. [PubMed: 8616858]
20. Anisimov VN, Ukraintseva SV, Yashin AI. Cancer in rodents: does it tell us about cancer in humans? *Nat Rev Cancer*. 2005; 5:807–19. [PubMed: 16195752]
21. Marino P, Pampallona S, Preatoni A, Cantoni A, Invernizzi F. Chemotherapy vs supportive care in advanced non-small-cell lung cancer. Results of a meta-analysis of the literature. *Chest*. 1994; 106:861–5. [PubMed: 7521815]
22. Ramalingam S, Belani C. Systemic chemotherapy for advanced non-small cell lung cancer: recent advances and future directions. *Oncologist*. 2008; 13 (Suppl 1):5–13. [PubMed: 18263769]
23. Horn L, Sandler AB. Emerging data with antiangiogenic therapies in early and advanced non-small-cell lung cancer. *Clin Lung Cancer*. 2009; 10 (Suppl 1):S7–16. [PubMed: 19362948]
24. Herbst RS, Madden TL, Tran HT, Blumenschein GR Jr, Meyers CA, Seabrooke LF, Khuri FR, Pudevalli VK, Allgood V, Fritsche HA Jr, Hinton L, Newman RA, et al. Safety and pharmacokinetic effects of TNP-470, an angiogenesis inhibitor, combined with paclitaxel in patients with solid tumors: evidence for activity in non-small-cell lung cancer. *J Clin Oncol*. 2002; 20:4440–7. [PubMed: 12431966]
25. Voskoglou-Nomikos T, Pater JL, Seymour L. Clinical predictive value of the in vitro cell line, human xenograft, and mouse allograft preclinical cancer models. *Clin Cancer Res*. 2003; 9:4227–39. [PubMed: 14519650]

26. Johnson JI, Decker S, Zaharevitz D, Rubinstein LV, Venditti JM, Schepartz S, Kalyandrug S, Christian M, Arbuck S, Hollingshead M, Sausville EA. Relationships between drug activity in NCI preclinical in vitro and in vivo models and early clinical trials. *Br J Cancer*. 2001; 84:1424–31. [PubMed: 11355958]
27. Zitvogel L, Apetoh L, Ghiringhelli F, Kroemer G. Immunological aspects of cancer chemotherapy. *Nat Rev Immunol*. 2008; 8:59–73. [PubMed: 18097448]
28. Suggitt M, Bibby MC. 50 years of preclinical anticancer drug screening: empirical to target-driven approaches. *Clin Cancer Res*. 2005; 11:971–81. [PubMed: 15709162]
29. Fiebig HH, Schuler J, Bausch N, Hofmann M, Metz T, Korrat A. Gene signatures developed from patient tumor explants grown in nude mice to predict tumor response to 11 cytotoxic drugs. *Cancer Genomics Proteomics*. 2007; 4:197–209. [PubMed: 17878523]
30. Fiebig, HH. Human tumor xenografts: predictivity, characterization and discovery of new anticancer agents. In: Fiebig, HH.; Burger, AM., editors. *Relevance of tumor models for anticancer drug development*. Basel, Switzerland: Karger; 1999. p. 29-50.
31. Dong Z, Radinsky R, Fan D, Tsan R, Bucana CD, Wilmanns C, Fidler IJ. Organ-specific modulation of steady-state mdr gene expression and drug resistance in murine colon cancer cells. *J Natl Cancer Inst*. 1994; 86:913–20. [PubMed: 7910854]
32. Killion JJ, Radinsky R, Fidler IJ. Orthotopic models are necessary to predict therapy of transplantable tumors in mice. *Cancer Metastasis Rev*. 1998; 17:279–84. [PubMed: 10352881]
33. Vantyghem SA, Wilson SM, Postenka CO, Al-Katib W, Tuck AB, Chambers AF. Dietary genistein reduces metastasis in a postsurgical orthotopic breast cancer model. *Cancer Res*. 2005; 65:3396–403. [PubMed: 15833874]
34. Thalheimer A, Otto C, Bueter M, Illert B, Gattenlohner S, Gasser M, Meyer D, Fein M, Germer CT, Waaga-Gasser AM. The intraportal injection model: a practical animal model for hepatic metastases and tumor cell dissemination in human colon cancer. *BMC Cancer*. 2009; 9:29. [PubMed: 19166621]
35. Demicheli R, Retsky MW, Hrushesky WJ, Baum M. Tumor dormancy and surgery-driven interruption of dormancy in breast cancer: learning from failures. *Nat Clin Pract Oncol*. 2007; 4:699–710. [PubMed: 18037874]
36. Hedley BD, Chambers AF. Tumor dormancy and metastasis. *Adv Cancer Res*. 2009; 102:67–101. [PubMed: 19595307]
37. Piedbois P, Buyse M. Endpoints and surrogate endpoints in colorectal cancer: a review of recent developments. *Curr Opin Oncol*. 2008; 20:466–71. [PubMed: 18525345]
38. Gill S, Sargent D. End points for adjuvant therapy trials: has the time come to accept disease-free survival as a surrogate end point for overall survival? *Oncologist*. 2006; 11:624–9. [PubMed: 16794241]
39. Fleming TR. Objective response rate as a surrogate end point: a commentary. *J Clin Oncol*. 2005; 23:4845–6. [PubMed: 15955898]
40. Sottnik JL, Duval DL, Ehrhart EJ, Thamm DH. An orthotopic, postsurgical model of luciferase transfected murine osteosarcoma with spontaneous metastasis. *Clin Exp Metastasis*. 27:151–60. [PubMed: 20213324]
41. Kim SH, Cho BC, Choi HJ, Chung KY, Kim DJ, Park MS, Kim SK, Chang J, Shin SJ, Sohn JH, Kim JH. The number of residual metastatic lymph nodes following neoadjuvant chemotherapy predicts survival in patients with stage III NSCLC. *Lung Cancer*. 2008; 60:393–400. [PubMed: 18155802]

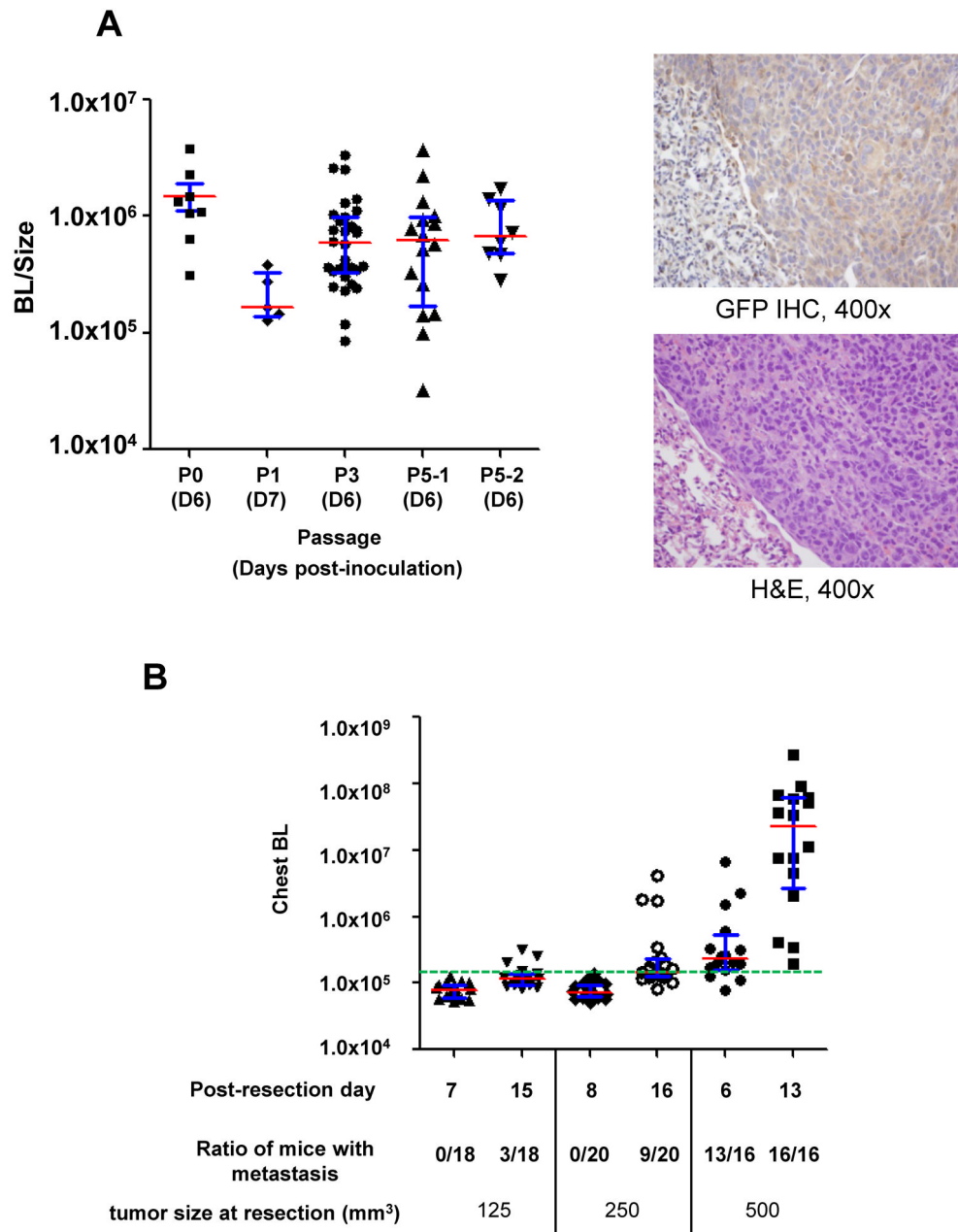


Figure 1. Generation of a syngeneic mouse model of spontaneous metastasis with uniformly-labeled LLCCom tumors

(A) *Left panel*, reporter activity in the labeled LLCCom was consistently maintained throughout *in vivo* passage. BL/size, normalized reporter activity in tumors; P0–P5, number of passage in mice (see text). *Right panels*, GFP expression (brownish cytoplasmic staining, upper panel) and the corresponding hematoxylin and eosin (H&E) staining pattern (lower panel) in a representative pulmonary metastatic LLCCom nodule (400x). Normal lung tissue shows only background GFP staining. (B) Effect of resection size of subcutaneous tumor on the occurrence of pulmonary metastasis. Subcutaneous LLCCom tumors were resected at indicated sizes, and post-resection changes of chest BL from pulmonary metastases in each group at indicated times are shown. Green dashed line, macrometastatic threshold (1.5×10^5)

photon/sec; see Fig. 2B and text). For both diagrams: red bar, median; blue whisker, interquartile range.

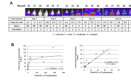


Figure 2. Quantitative monitoring of metastatic progression in LLCom model

(A) Post-resection metastatic progression in LLCom model. Upper panel, BL images of mice *in vivo* at indicated days after primary tumor resection. Lower panel, the corresponding metastatic progression score (1, minimal; 2, mild; 3, moderate; 4 marked) and disease pattern (MF, multifocal; D, diffuse) from pathological analysis. (B) The lung sections from (A) were digitally analyzed to quantify the overall areas of tumor nodules, and the correlation between tumor area and chest BL was examined by regression analysis. *Left panel*, distribution of chest BL and tumor area of all 17 mice. *Right panel*, in mice in which chest BL $< 5 \times 10^7$ (13 of 17 mice) chest BL significantly correlated with the tumor area in a linear manner. The linearity equation and regression coefficient (R^2) are shown.

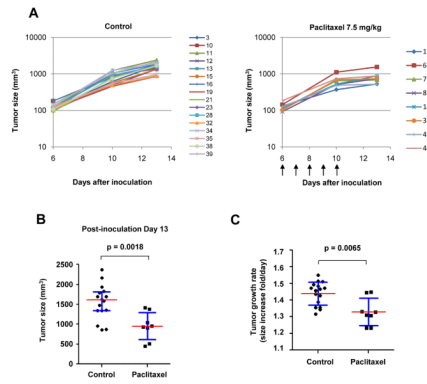


Figure 3. Efficacious paclitaxel treatment delays the growth of subcutaneous tumors

When subcutaneous LLC_{om} tumors reached 125 mm³, mice were randomized to receive vehicle solution (control) or 7.5 mg/kg of paclitaxel (treated). Tumor growth curves of individual mice in control or treated group are shown in (A) and (B), respectively. Marker indicating the mouse number is listed to the right of each chart. Arrows under (B), dosing schedule. (C) At day 13, tumor size in treated group is significantly smaller than that in control group. (D) Growth rate in the treated group was significantly reduced relative to the control group. The tumor sizes at various time points were converted to “fold-increased per day”. The p value in (C) and (D) was obtained by unpaired t-test.

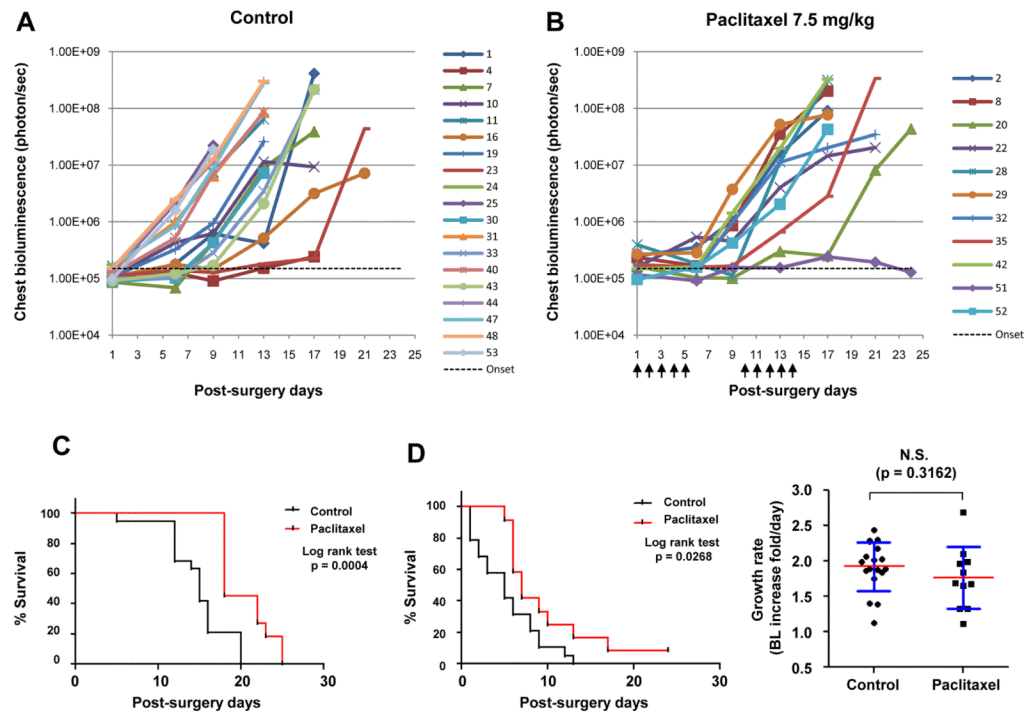


Figure 4. Efficacious paclitaxel treatment prolonged disease-free and overall survival in a spontaneous metastasis model without significant effect on disease growth rate
 After resection of the subcutaneous LLC_{om} tumors at 500 mm³, mice were randomized to receive vehicle solution (control) or 7.5 mg/kg of paclitaxel (treated). By BL monitoring, metastatic growth curves of individual mice in control and treated group are shown in (A) and (B), respectively. Markers at the right of the chart indicate individual mouse data. Arrows under (B), dosing schedule; green dash line, macrometastatic threshold. (C) Kaplan-Meier analysis showing that post-surgery overall survival (OS) and disease-free survival (DFS) was significantly prolonged in treated groups relative to control group. (D) The treatment had no significant effect on the growth rate of pulmonary metastasis. For each mouse, time course of chest BL was converted to “fold-increased per day”. N.S., not significant. The p value was obtained by unpaired t-test.

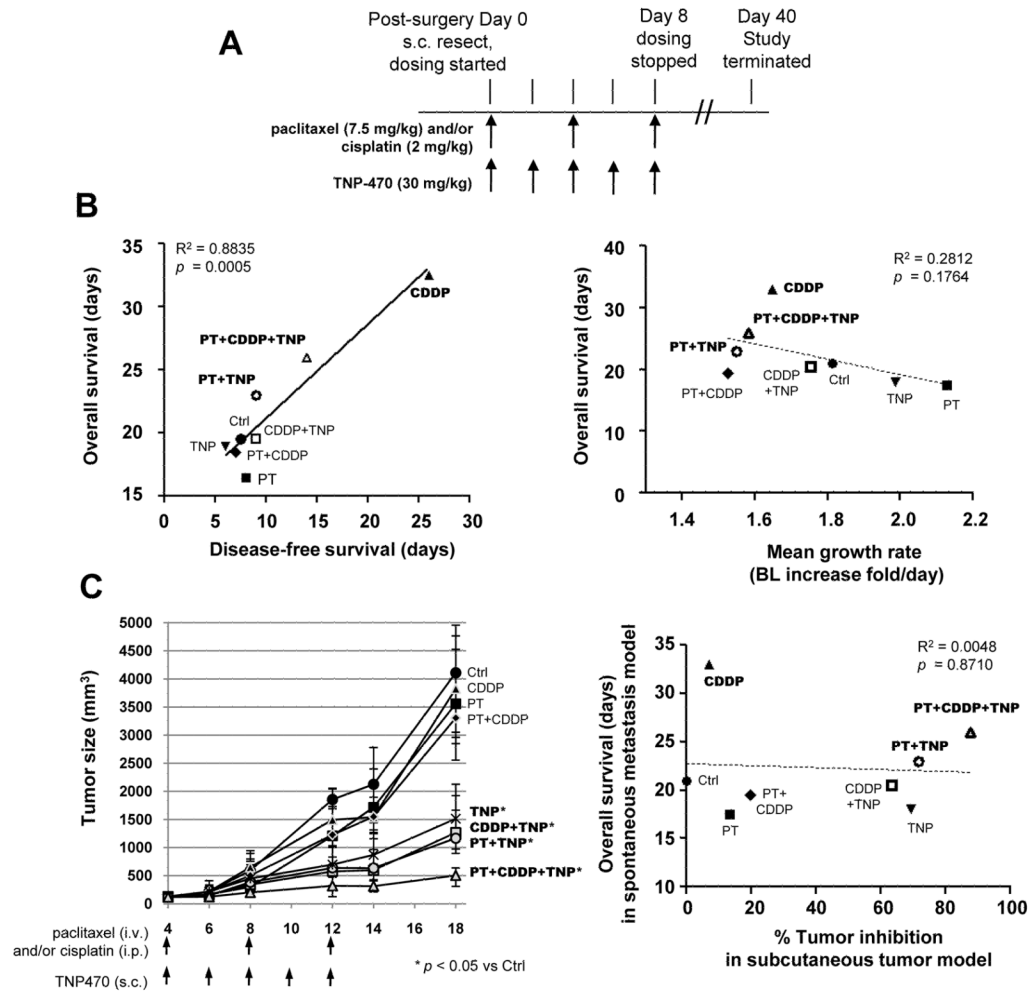


Figure 5. Prognosis in the LLCCom model of spontaneous metastasis is determined by disease-free survival, not growth rate

(A) Design of the adjuvant chemotherapeutic setting. After the resection of subcutaneous tumors (post-surgery Day 0), mice were randomized to receive vehicle solution (control), chemotherapeutic agents, or their combinations, followed by BL monitoring for therapeutic responses. In combination treatment, individual drugs were given at the same dose and schedule as indicated. (B) *Left panel*, regression analysis showing that DFS time is highly correlated with OS for adjuvant chemotherapeutic setting. *Right panel*, no significant correlation was found between OS and average growth rate of pulmonary metastasis (calculated in the same way as Fig. 4D). In both panels, regression coefficient (R^2) and p value are shown. PT, paclitaxel; CDDP, cisplatin; TNP, TNP470. (C) *Left panel*, effect of drugs and combinations on the subcutaneous LLCCom tumors. Treatment was initiated when the subcutaneous tumors reached 125 mm^3 with the indicated agents and schedules. Doses of the agents were the same as in Fig. 5A. For each time point, the median size of control and treated groups are shown. Whiskers, interquartile range. p-value was determined by One-way ANOVA. Tumor inhibition ratio (see Supplementary Method) at day 18 was calculated for each treatment. *Right panel*, no correlation existed between tumor inhibition ratio in subcutaneous tumor model (Fig. 5C) and OS in post-surgery metastasis model (Fig. 5B).

Table 1

Correlation between mouse chest BL intensity and pulmonary metastasis progression

Chest BL	Corresponding Lung Pathology	Score
$< 1.5 \times 10^5$	No overt pathology	-
$1.5 \times 10^5 - 1 \times 10^6$	Single or multifocal lesions	1-2
$1 \times 10^6 - 5 \times 10^7$	Mostly multifocal	3-4
$> 5 \times 10^7$	Diffuse	4